ChemComm

Accepted Manuscript

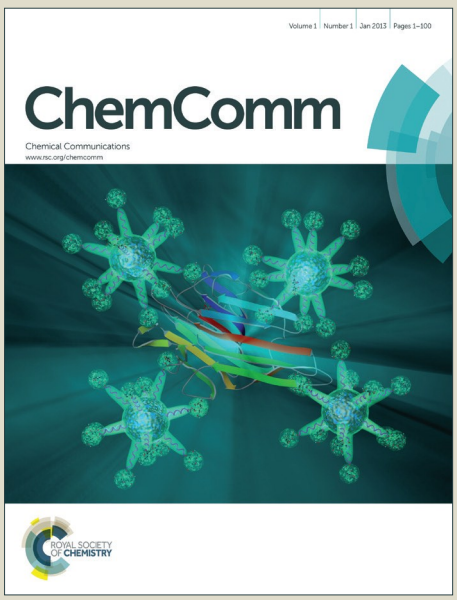

ROYAL SOCIETY OF CHEMISTRY

www.rsc.org/chemcomm

Cite this: DOI: 10.1039/c0xx00000x

www.rsc.org/xxxxxx

ARTICLE TYPE

Aggregates of Silicon Quantum Dots as a Drug Carrier: Selective Intracellular Drug Release Based on pH-responsive Aggregation/Dispersion

Seiichi Ohta,*‡ Kentaro Yamura, Susumu Inasawa‡ and Yukio Yamaguchi

Received (in XXX, XXX) Xth XXXXXXXXX 20XX, Accepted Xth XXXXXXXXX 20XX
DOI: 10.1039/b000000x

Using amine-modified silicon quantum dots (Si-QDs) with visible photoluminescence as a building block, drug-loaded Si-QD aggregates were assembled. The aggregates were designed to break down in response to the endosomal pH decrease, which enabled selective intracellular release of the loaded drugs.

Fluorescent imaging is now recognized as a powerful tool for diagnosis of diseases, such as cancer[1] and arteriosclerosis.[2] Combined with drug delivery systems, it is expected to enable multimodal treatment consisting of improved detection, site-specific therapy, and long-term monitoring (often referred to as theranostics).[3,4] As a photoluminescent imaging agent, silicon quantum dots (Si-QDs) have attracted significant attention because they are more resistant to photo bleaching than organic dyes and less cytotoxic when compared with other, conventional quantum dots, such as CdSe and CdTe.[5-7] The applicability of Si-QDs as imaging agents has been examined both *in vitro*[8-13] and *in vivo*,[14,15] and diagnostic imaging of cancer and the sentinel lymph node has been reported.[6] However, although drug conjugation to Si-QD was recently reported,[16-17] the method for loading drugs in Si-QDs and controlling the release of the loaded drugs has not been established.

In this study, we developed drug-loaded aggregates of Si-QDs, which were designed to release drugs at low pH. Our concept is schematically shown in Fig. 1. The drugs are loaded into Si-QD aggregates that have diameters of ~100 nm. Because of their size, they are internalized by cells via endocytosis and transported to late endosomes/lysosomes,[9,12] in which, the pH is lower than the extracellular environment (the pH change is normally from 7.5 to ca. 5.0). In response to this pH change, the aggregates break down into several species with smaller size and the drugs are released. To realize this selective intracellular drug release, we employed a surface modification of amine molecules on Si-QDs. It was recently reported that cysteamine-modified nanoparticles showed reversible aggregation/dispersion against a change in pH;[18] they formed aggregates by inter-particle hydrogen bond formation at neutral pH, whereas the aggregates broke down owing to electrostatic repulsive forces exerted on the particles by protonation of surface amines under an acidic environment. We applied this amine-induced aggregation/dispersion mechanism into our system to achieve selective intracellular drug release inside acidic late endosomes/lysosomes.

Si-QDs were synthesized via plasma-assisted decomposition of $SiBr_4$, as described in our previous report.[19] The diameter of the synthesized particles was 3.5 ± 2.2 nm. As a surface modification agent we chose allylamine whose pK_b (4.5) is near the endosomal pH. The surface of the Si-QDs was then modified with allylamine via a Pt-catalyzed hydrosilylation reaction, as previously described.[8-9] The covalent bond formation between allylamine molecules and Si-QD surface was confirmed by ATR-FTIR (Fig. S1, ESI†). The amine-terminated Si-QDs were dispersed in aqueous media and showed photoluminescence (PL) with a PL emission peak of 450 nm when excited at 360 nm (Fig. S2, ESI†). The quantum yield was 18%. We chose doxorubicin (DOX) as a model drug because of its clinical use in cancer chemotherapy and its affinity to the amine-terminated surface via NH···N hydrogen bond formation.[20-21] DOX was added to the amine-terminated Si-QD dispersion at pH 3, because the Si-QDs were supposed to be stabilized by electrostatic repulsion via the protonated surface amines. The solution pH was gradually increased to 7.5 by the addition of NaOH to weaken the electrostatic repulsion forces on Si-QDs via deprotonation of the surface amines. In this pH increase step, Si-QDs formed aggregates with a diameter of ca. 180 nm and a polydispersity index (PDI) of 0.184, as measured by dynamic light scattering (DLS). The aggregates kept their size almost constant at least one month (Fig. S3, ESI†). In addition, it was found that the size of the formed aggregates decreased at high temperature (Fig. S4, ESI†), which is known to inhibit the hydrogen bond formation.[18] This indicates that NH···N hydrogen bonds among surface-amine groups on Si-QDs contribute to the formation of aggregates of Si-QDs. DOX molecules were loaded into the aggregates through this aggregation process. The amount of loaded DOX was 8.3 wt% (mass of loaded DOX/mass of Si-QDs), as determined by optical absorbance at 485 nm from DOX. Physical entrapment into inter-particle spaces, NH···N hydrogen bond formation with surface amines on Si-QDs, or hydrophobic interaction with un-modified Si-QD surface are considered to be possible reasons for the DOX loading.

The average size of the formed aggregates decreased when exposed to acidic conditions as shown in Fig. 2a (for results in basic conditions, see Fig. S5, ESI†). The size change usually took around 30 min (Fig. S6, ESI†). One main feature is that reduction

Cite this: DOI: 10.1039/c0xx00000x

www.rsc.org/xxxxxx

ARTICLE TYPE

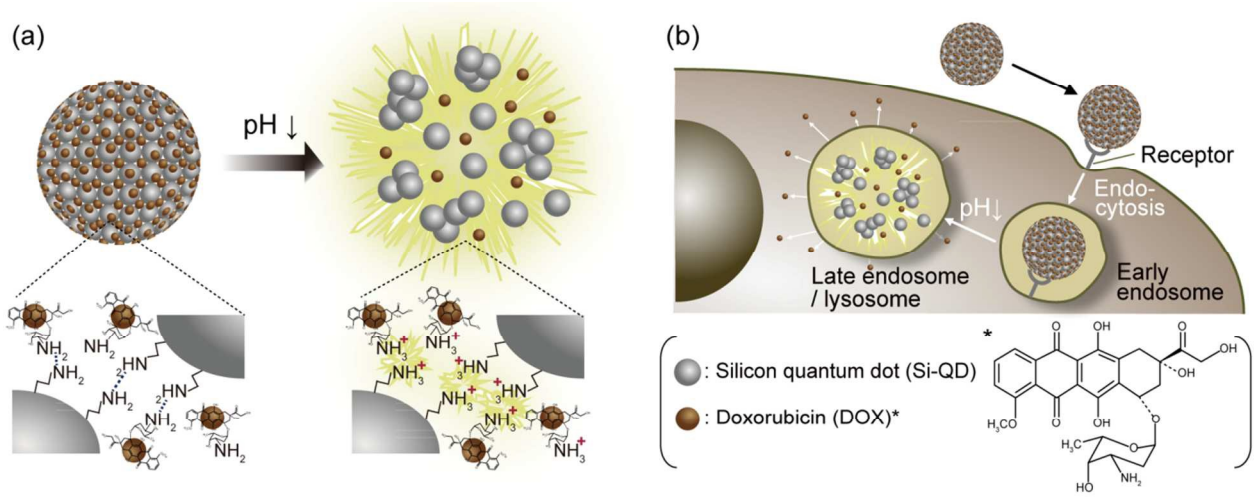

Fig. 1 Schematic illustration of (a) pH-triggered re-dispersion of the DOX-loaded Si-QD aggregates and (b) selective intracellular DOX release from the Si-QD aggregates.

of the aggregate size was accompanied by an increase in the zeta potential. The increase in zeta potential was caused by the protonation of surface amines on Si-QDs at low pH, which introduced an electrostatically repulsive force among Si-QDs and therefore the initial aggregates broke down into several species with smaller size. Protonation/deprotonation of amines responsive to the surrounding solution pH represents a key issue to controlling the size of the aggregates. It should be noted that even at low pH, Si-QDs were not necessarily mono-dispersed. Irreversible aggregation during the synthetic procedures and/or electrostatic interaction between surface amines and inevitably formed surface oxide layer could be the reason for that. Optimization of the surface chemistry on Si-QDs could improve the controllability of the aggregate size.

Loaded DOX was released from the aggregates under acidic conditions. Fig. 2b shows DOX release profiles from the Si-QD aggregates at two different solution pH values. At neutral pH (pH 7.5), at most ca. 5% of the initially loaded DOX was released from the aggregates. Conversely, pronounced DOX release was observed under the acidic environment (pH 5.0 and 2.6). At pH 5.0, which is close to endosomal pH, the total amount of released DOX after 40 h was ca. 4-fold larger than that at neutral pH. This "ON/OFF" contrast is comparable to or even higher than other polymer-based stimuli-responsive systems.[22,23] The largest amount of DOX was released within the initial 10 h, which was a slower process than the size change of Si QDs (Fig. S6, ESI†). From these results, dynamics of DOX release is suggested as follows. At the time when Si-QDs broke down, most of the loaded DOX still remained loaded into the broken species (with smaller size). Afterwards, DOX was gradually released from the broken-aggregates, the speed and amount of which was higher than that at pH 7 due to the increased surface area and/or reduced DOX affinity of the Si-QDs owing to the protonation of amines.

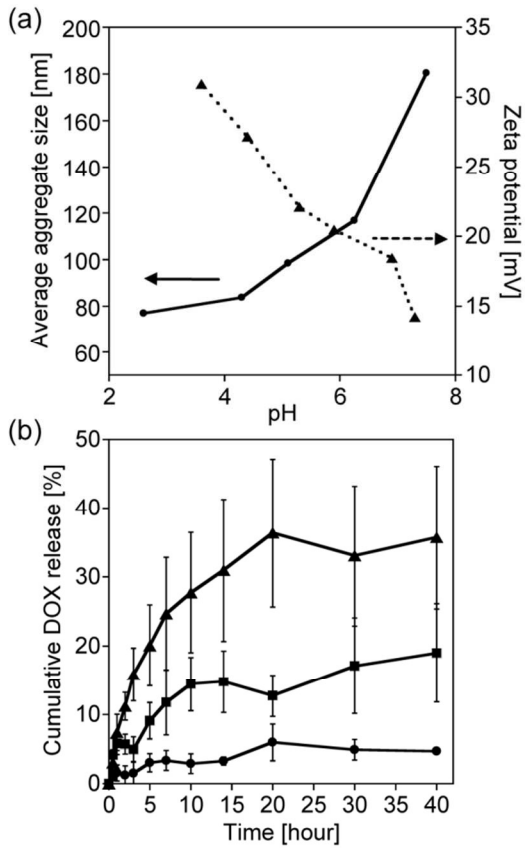

Fig. 2 (a) Effect of pH on size (circles) and zeta potential (triangles) of the Dox-loaded Si-QD aggregates. (b) Dox release profiles from the Si-QD aggregates at different pH values. The fraction of released Dox to the total amount of loaded Dox is plotted against time. Circles, squares and triangles represent the results at pH 7.5, 5.0, and 2.6, respectively.

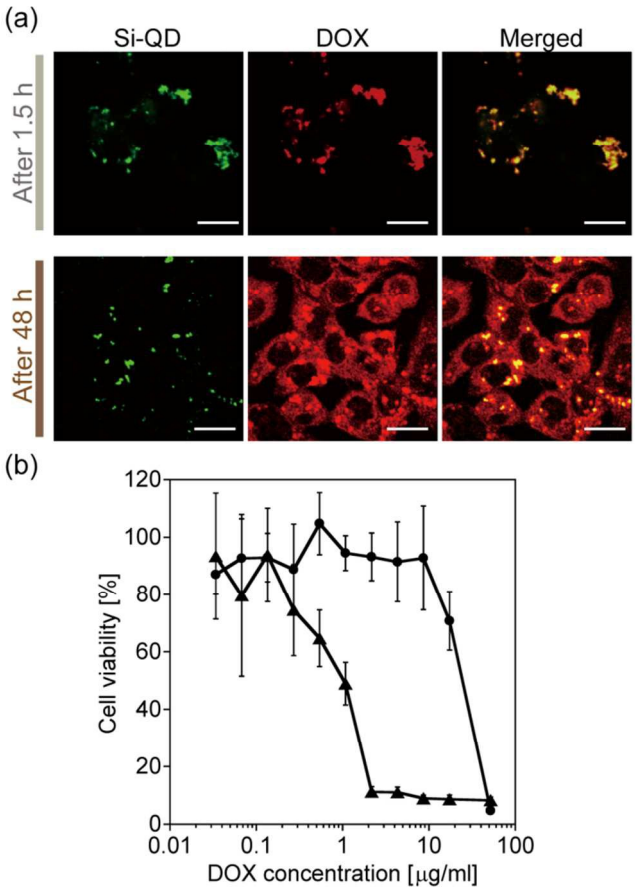

Fig. 3 (a) Confocal microscope images of HepG2 cells exposed to the Dox-loaded Si-QD aggregates for 1.5 h (the top row) and 48 h (the bottom row). In each row, the left and central image represents the fluorescent image from Si-QDs and Dox, and the right image represents the merged image. The scale bar is 20 μm. (b) Cell viability assay for HepG2 cells exposed to the Dox-loaded Si-QD aggregates (circles) and free Dox (triangles).

The selective intracellular drug release property of the DOX-loaded Si-QD aggregates was examined *in vitro* using HepG2 liver carcinoma cells. The aggregate dispersion (100 μg/ml) was exposed to HepG2 cells, and the intracellular distribution of both Si-QDs and DOX was tracked by a confocal laser scanning microscope. Fig. 3a shows the intracellular distribution of Si-QDs and DOX after 1.5 and 48 h exposure. Si-QDs and DOX are depicted in green and red, respectively, so that co-localization of Si-QDs and DOX is seen in yellow in the merged images. After exposure for 1.5 h, Si-QDs were internalized by HepG2 cells and observed as a punctuate pattern. This punctuate pattern was confirmed to be late endosomes/lysosomes by co-localization experiments with LysoTracker (Fig. S7, ESI†). Almost all loaded DOX was co-localized with Si-QDs, suggesting that loaded DOX was hardly released from the internalized aggregates at this stage (i.e., 1.5 h). However, while Si-QDs remained localized in a punctuate pattern, DOX was widely distributed in the cytoplasm after 48 h, suggesting that DOX was released from the Si-QD aggregates following sufficient time exposure (i.e., 48 h). In addition, though signal from DOX is weak in the nuclear region, it not necessarily means that few DOX is transported into the cell nuclei because DOX fluorescence is quenched by the intercalation into DNA.[25] In fact, similar confocal microscopic images were also reported in previous reports which used nanoparticles as carrier of DOX.[26] These results suggest that the DOX-loaded Si-QD aggregates release DOX only following cellular uptake, which results in selective intracellular DOX release.

The growth-inhibition effect of the DOX-loaded Si-QD aggregates against HepG2 cells was also examined using a cell viability assay. The DOX-loaded Si-QD aggregates, Si-QD aggregates without DOX loading, and free DOX were exposed to HepG2 cells at various concentrations for 48 h, and then cell viability was evaluated using a Cell Counting Kit-8. While Si-QD aggregates without DOX did not show any significant cytotoxicity over the examined particle concentration range (Fig. S8, ESI†), the DOX-loaded Si-QD aggregates exhibited clear growth-inhibition against HepG2 cells, indicating the applicability of these aggregates as a chemotherapeutic agent. However, it should be noted that the IC_{50} value for the DOX-loaded Si-QD aggregates was higher than that for free DOX (though similar with other DOX delivery systems using hydrogen bonding[20,21]), implying less drug efficacy of the DOX-loaded aggregates compared with free DOX. A reason for this reduced efficacy is the incomplete release of DOX from the Si-QD aggregates at the endosomal pH. Although good ON/OFF contrast was observed in Fig. 2b, ca. 80% of the initially loaded DOX was not released from Si-QD aggregates at pH 5.0, which is comparable to the endosomal pH. More efficient use of the loaded DOX (e.g., optimization of the degree of amine modification on the Si-QD surface) could contribute to further improvements in the performance of Si-QD aggregates as a drug carrier.

One unique feature of our methodology is that Si-QDs are used in an aggregated form and the control of drug release is based on their aggregation/dispersion, which is induced by the protonation of surface amines. It has been reported that few tens of nanometers to hundreds of nanometers are a preferable size for nanoparticles to reduce clearance and improve accumulation within tumors (EPR effect).[27,28] However, semiconductor QDs generally show unique properties only when their diameters are in the range of single nanometers. Thus, their use in an aggregated or assembled form is a practical approach for biomedical applications.[5,9,29,30] However, if Si-QDs remain aggregated at the time of drug release, even though drugs are released from Si-QD surface the release of drugs would be severely restricted by the entrapment of the drugs within the inter-particle space inside the aggregates. Therefore, the controlled drug release based on aggregation/dispersion of Si-QDs is a promising concept for achieving efficient site-specific treatment while maintaining excellent optical properties of Si-QDs. Our proposed concept should be applicable to semiconductor QDs and other nanoparticle-based systems, such as magnetic nanoparticles or gold nanoparticles.

In conclusion, we have developed DOX-loaded Si-QD aggregates in this study. These aggregates disintegrated into smaller species in response to a decrease in the surrounding pH and protonation of surface amines, followed by a subsequent release of loaded DOX. Additionally, we demonstrated that Si-QD aggregates were internalized by HepG2 cells and loaded DOX was released inside the cells, thus the aggregates function

as an anticancer agent carrier. This is the first report on the use of Si-QDs as a stimuli-responsive drug carrier. Combined with low cytotoxicity and the excellent optical properties of Si-QDs, the DOX-loaded Si-QD aggregates should enable multimodal treatment consisting of both diagnosis and therapy.

We thank Prof. T. Ito for useful discussion and Dr. P. Shen for the experimental set up for the synthesis of Si-QDs. We are also grateful to Drs. S. Hanada and K. Yamamoto for access to the microplate reader. S. Ohta is the recipient of a Research Fellowship from the Japan Society for the Promotion of Science (JSPS). This work was partially supported by the Konica Minolta Science and Technology Foundation.

Notes and references

Department of Chemical System Engineering, The University of Tokyo, 7-3-1 Hongo, Bunkyo-ku, Tokyo 113-8656 Japan.
E-mail: s-ohta@chemsys.t.u-tokyo.ac.jp

† Electronic Supplementary Information (ESI) available: [details of any supplementary information available should be included here]. See DOI: 10.1039/b000000x/

‡ Current address for S. Ohta: Center for Disease Biology and Integrative Medicine, Faculty of Medicine, The University of Tokyo, 7-3-1 Hongo, Bunkyo-ku, Tokyo 113-0033 Japan. Current address for S. Inasawa: Graduate School of Bio-Applications and Systems Engi-neering, Tokyo University of Agriculture and Technology, 2-24-16 Nakacho, Koganei, Tokyo 184-8588 Japan.

1 Y. Urano, D. Asanuma, Y. Hama, Y. Koyama, T. Barrett, M. Kamiya, T. Nagano, T. Watanabe, A. Hasegawa, P. L. Choyke and H. Kobayashi, *Nat. Med.* 2009, **15**, 104-109.
2 J. Ding, Y. Wang, M. Ma, Y. Zhang, S. Lu, Y. Jiang, C. Qi, S. Luo, G. Dong, S. Wen, Y. An and N. Gu, *Biomaterials* 2013, **34**, 209-216.
3 J. Xie, S. Lee and X. Chen, *Adv. Drug Deliv. Rev.* 2010, **62**, 1064-1079.
4 A. Modak, A. K. Barui, C. R. Patra and A. Bhaumik, *Chem. Commun.* 2013, **49**, 7644-7646.
R. Hu, X. Zhang, Z. Zhao, G. Zhu, T. Chen, T. Fu and W. Tan, *Angew. Chem. Int. Ed.* 2014, **53**, 5821-5826.
5 Y. He, Z.-H. Kang, Q.-S. Li, C. H. A. Tsang, C.-H. Fan and S.-T. Lee, *Angew. Chem. Int. Ed.* 2009, **48**, 128-132.
6 F. Erogbogbo, K.-T. Yong, I. Roy, R. Hu, W.-C. Law, W. Zhao, H. Ding, F. Wu, R. Kumar, M. T. Swihart and P. N. Prasad, *Acs Nano* 2011, **5**, 413-423.
7 P. Shen, S. Ohta, S. Inasawa and Y. Yamaguchi, *Chem. Commun.* 2011, **47**, 8409-8411.
8 J. H. Warner, A. Hoshino, K. Yamamoto and R. D. Tilley, *Angew. Chem. Int. Ed.* 2005, **44**, 4550-4554.
9 S. Ohta, P. Shen, S. Inasawa and Y. Yamaguchi, *J. Mater. Chem.* 2012, **22**, 10631-10638.
10 C. Tu, X. Ma, P. Pantazis, S. M. Kauzlarich and A. Y. Louie, *J. Am. Chem. Soc.* 2010, **132**, 2016-2023.
11 Y. Zhong, F. Peng, X. Wei, Y. Zhou, J. Wang, X. Jiang, Y. Su, S. Su, S.-T. Lee and Y. He, *Angew. Chem. Int. Ed.* 2012, **51**, 8485-8489.
12 S. Ohta, S. Inasawa and Y. Yamaguchi, *Biomaterials* 2012, **33**, 4639-4645.
13 K. Sato, S. Yokosuka, Y. Takigami, K. Hirakuri, K. Fujioka, Y. Manome, H. Sukegawa, H. Iwai and N. Fukata, *J. Am. Chem. Soc.* 2011, **133**, 18626-18633.
14 C. M. Hessel, M. R. Rasch, J. L. Hueso, B. W. Goodfellow, V. A. Akhavan, P. Puvanakrishnan, J. W. Tunnel and B. A. Korgel, *Small* 2010, **6**, 2026-2034.
15 C. Tu, X. Ma, A. House, S. M. Kauzlarich, and A. Y. Louie, *ACS Med. Chem. Lett.* 2011, **2,** 285-288.
16 Q. Wang, Y. Bao, J. Ahire and Y. Chao, *Adv. Healthc. Mater.* 2013, **2**, 459-466.
17 S. Hanada, K. Fujioka, Y. Futamura, N. Manabe, A. Hoshino and K. Yamamoto, *Int. J. Mol. Sci.* 2013, **14**, 1323-1334.
18 J. Liu, X. Yang, K. Wang, R. Yang, H. Ji, L. Yang and C. Wu, *Chem. Commun.* 2011, **47**, 935-937.
19 P. Shen, N. Uesawa, S. Inasawa and Y. Yamaguchi, *J. Mater. Chem.* 2010, **20**, 1669-1675.
20 S. H. Kim, J. P. Tan, F. Nederberg, K. Fukushima, J. Colson, C. Yang, A. Nelson, Y. Y. Yang and J. L. Hedrick, *Biomaterials* 2010, **31**, 8063-8071.
21 J. P. Tan, S. H. Kim, F. Nederberg, K. Fukushima, D. J. Coady, A. Nelson, Y. Y. Yang and J. L. Hedrick, *Macromol. Rapid Commun.* 2010, **31**, 1187-1192.
22 E. S. Lee, K. T. Oh, D. Kim, Y. S. Youn and Y. H. Bae, *J. Control. Release* 2007, **123**, 19-26.
23 N. Singh, A. Karambelkar, L. Gu, K. Lin, J. S. Miller, C. S. Chen, M. J. Sailor and S. N. Bhatia, *J. Am. Chem. Soc.* 2011, **133**, 19582-19585.
24 T. Ito, I. P. Fraser, Y. Yeo, C. B. Highley, E. Bellas and D. S. Kohane, *Biomaterials* 2007, **28**, 1778-1786.
25 D. Agudelo, P. Bourassa, G. Bérubé, and H.-A. Tajmir-Riahi, *Int. J. Biol. Macromol.* 2014, **66**, 144-150.
26 X. Shuai, H. Ai, N. Nasongkla, S. Kim, and J. Gao, *J. Control. Release* 2004, **98**, 415-426.
27 H. Cabral, Y. Matsumoto, K. Mizuno, Q. Chen, M. Murakami, M. Kimura, Y. Terada, M. R. Kano, K. Miyazono, M. Uesaka, N. Nishiyama and K. Kataoka, *Nat. Nanotechnol.* 2011, **6**, 815-823.
28 H. Choi, W. Liu, P. Misra, E. Tanaka, J. P. Zimmer, B. I. Ipe, M. G. Bawendi and J. V. Frangioni, *Nature Biotechnol.* 2007, **25**, 1165-1170.
29 L. Y. Chou, K. Zagorovsky and W. C. W. Chan, *Nat. Nanotechnol.* 2014, **9**, 148-155.
30 J. H. Park, G. von Maltzahn, L. L. Zhang, M. P. Schwartz, E. Ruoslahti, S. N. Bhatia and M. J. Sailor, *Adv. Mater.* 2008, **20**, 1630-1635.

(Table of contents entry)

Aggregates of Silicon Quantum Dots as a Drug Carrier: Selective Intracellular Drug Release Based on pH-responsive Aggregation/Dispersion

Seiichi Ohta*, Kentaro Yamura, Susumu Inasawa and Yukio Yamaguchi

Department of Chemical System Engineering, The University of Tokyo,
7-3-1 Hongo, Bunkyo-ku, Tokyo, 113-8656, Japan
* E-mail: s-ohta@chemsys.t.u-tokyo.ac.jp

Table of contents entry

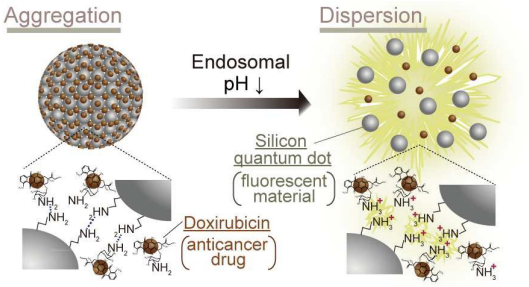

A novel, controlled drug-release system was developed based on aggregation/dispersion of silicon quantum dots (Si-QDs) in response to a change in the pH environment.